

# Role of ultrasonic irradiation and Thiourea on the synthesis of PbS nanocrystals

V. PARASHAR<sup>\*a</sup>, S. K. PANDEY<sup>a</sup>, A. C. PANDEY<sup>a</sup>

<sup>a</sup>Nanophosphor Application Centre, Department of Physics, University of Allahabad, Allahabad-211002, India

A novel strategy is adopted for synthesis of PbS nanocrystals via ultrasonic irradiation method underlining the effect of acoustic cavitation phenomenon on crystallinity and particle size in presence of a thiourea. X-ray diffraction (XRD) measurements have shown formation of face-centered cubic rock-salt PbS structure with enhanced crystallinity as compared to other routes. Transmission electron microscopy (TEM) images have shown particles about 5 – 15 nm range that are smaller than its Bohr Exciton radius of 18 nm. Absorption spectra have shown narrow band-edge around 275 nm that confirmed its monodispersity and blue shift in comparison to bulk PbS. Photoluminescence spectra have shown sharp emission peak at 590 nm. A probable path for its formation and chemistry is discussed to understand the mechanism of this method.

(Received August 31, 2009; accepted November 22, 2009)

**Keywords:** PbS nanocrystals, Ultrasonication, Acoustic cavitation

## 1. Introduction

Ternary and quaternary semiconductor nanocrystals (~ 2 nm – 100 nm) of II-VI with unique optical and electrical properties currently being applied to a broad range of optoelectronic devices for example, LED's [1-3], single electron transistors [4], infrared detectors, infrared photo emitters and infrared sensors [5]. Semiconductor nanocrystals surface to volume ratio significantly defines its optoelectronic properties. In recent years, PbS nanostructures have attracted ample cognizance due to their versatile shapes, size and applications such as third order non-linear optical [7, 8] and non-ohmic electrical properties [9, 10]. PbS is a direct band gap II-VI semiconductor having a band gap of 0.41 eV with Bohr exciton radius of 18 nm; reduction of grain size to 2 nm increases its energy band gap to 5.4 eV. Further, modifying the surface of the nanocrystals increases their quantum efficiency as well as thermal stability. For instance, absorption and luminescent properties of surface capped PbS nanocrystals can be easily tuned by selecting appropriate matrix materials or organic solvents such as AOT [16], Alkanethiolate [17], PVA, DNA, and PMMA [18]. Solution-processed electronic and optoelectronic devices has a clear superiority over the conventional crystalline semiconductor devices in terms of easy synthesis, large device area, physical flexibility, and most importantly, low cost. With this in view we considered it worthwhile to explore how the optical properties of PbS nanocrystals can be adjusted by using acoustic cavitations in presence of a capping agent. The purpose of this paper is 2-fold: (1) to present a simple method of PbS nanocrystals synthesis and discuss its limitations, and (2) to describe their optical properties.

## 2. Experimental section

A simple wet co-precipitation chemical route was adopted for the synthesis of PbS nanoparticles. The

precursors, Lead acetate dihydrate ( $\text{CH}_3\text{COO}$ )<sub>2</sub>.Pb.2H<sub>2</sub>O, and Thiourea (NH<sub>2</sub>-CS-NH<sub>2</sub>) (of analytical grade) were used. Preheated 1.5 M thiourea was mixed drop wise to 0.1 M lead acetate under high energy ultrasonicator for about 2 hour (Fig. 1). Such synthesized PbS was precipitated out from solution, filtered and washed thrice with absolute ethanol and water and dried. The PbS powders were then subjected to various characterization techniques.

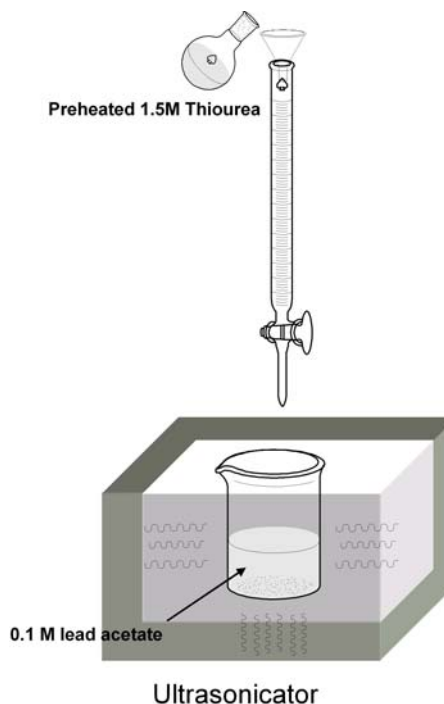


Fig. 1. Schematic diagram showing mode of Ultrasonication irradiation in Sonication bath.

### 3. Characterization technique

The crystal structure of PbS nanoparticles were characterized by Rigaku D/MAX-2200 H/PC X-Ray Diffractometer Cu K $\alpha$  ( $\lambda=1.54\text{\AA}$ ) radiation. Absorption spectra were recorded on Perkin Elmer Lamda-35 UV-Vis spectrometer. Photoluminescence spectra of synthesized materials were scanned from Perkin Elmer LS-55 spectrophotometer with the excitation source of 350 nm.

## 4. Result and discussion

### 4.1. X-Ray Diffraction Pattern

Fig. 2 shows the X-ray powder diffraction pattern of as prepared and sonicated PbS nanoparticles. The XRD peaks are broadened due to the nanocrystalline nature of the particles and from the XRD pattern of both sample, it is clear that these nanoparticles have face-centered cubic rock salt structure with planes at [111], [200], [220], [311] and [221] respectively. Traces of PbO or any other phase is absent and indicating the purity of samples. The crystallinity of XRD peaks of PbS nanoparticles synthesized in presence of ultrasonic irradiation are higher in comparison to synthesized in absence of ultrasonic irradiation. These results suggest that ultrasonic radiations played a decisive role in an augmentation of crystallinity of particles.

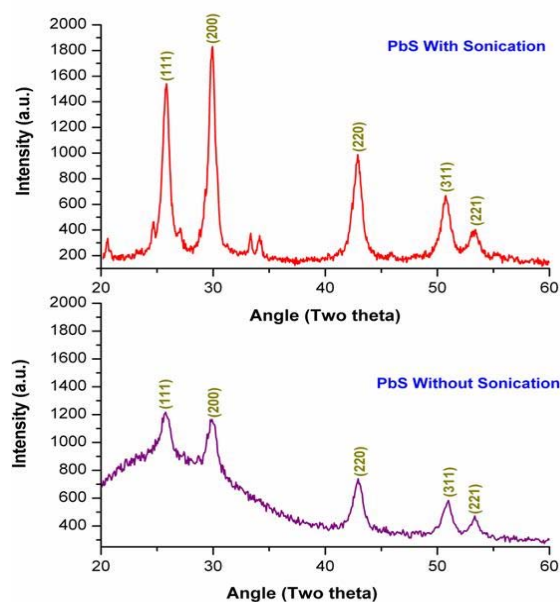


Fig. 2. X-Ray Different pattern of sonicated and pristine PbS nanoparticles.

Fig. 3 shows the transmission electron microscope [TEM] image of the PbS nanoparticles that divulge particle size is about 5–15 nm with diffused spherical morphology.

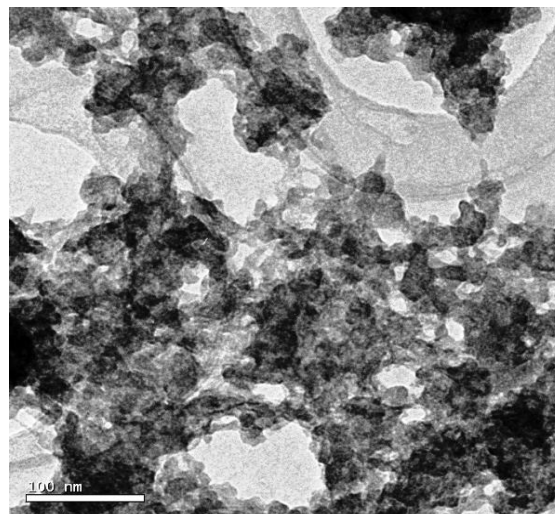


Fig. 3. TEM image of PbS nanoparticles synthesized by sonochemical method.

### 4.2 Absorption Spectra

The UV-Vis absorption spectra of the PbS nanocrystals prepared in with and without ultrasonic waves, were shown in Fig. 4. Since the size of particles (as evident from TEM image) were smaller than the Bohr exciton radius of PbS (18 nm), therefore they were subjugated to strong confinement effect. Following these reasons and also due to small effective mass of PbS, the spectra display a large blue shift in comparison to bulk PbS ( $E_g = 0.41$  eV). From absorption spectrum it is clear that band edge is very narrow in case of sonicated sample which confirms that the monodispersity of particles increases due to high energy ultrasonication.

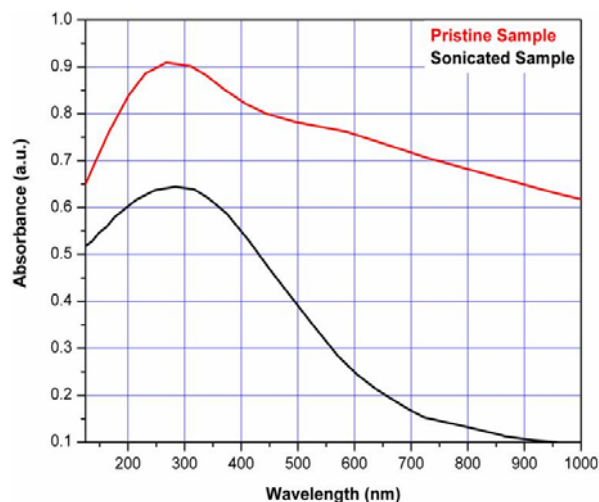


Fig. 4. UV-Visible absorption spectrum of sonicated PbS nanoparticles.

### 4.3 Photoluminescence Spectra

The photoluminescence emission spectra, shown in Fig. 5, were measured from 400 nm to 700 nm at the room temperature and the excitation wavelength was 350 nm. Fig. 5 shows that a sharp peak is positioned around 590 nm (2.11 eV) which appears after PbS nanoparticles produced under ultrasonicator. The energy transitions in both electron and hole levels of PbS nanocrystals were revealed in four major types, the  $S_e-S_h$ ,  $S_e-P_h$ ,  $P_e-S_h$  and  $P_e-P_h$  transitions [19]. In Fig. 5, the emission peak observed at 2.11 eV corresponds to the  $S_e-S_h$  transition which is a lowest energy exciton. The probable explanation about the energy gap of PbS shifts from 0.41 eV to 2.11 eV is indicative of the presence of the quantum confinement effect. Quantum confinement in the PbS nanocrystals results in discrete energy levels and increase in the effective band gap from the bulk value of 0.41 eV.

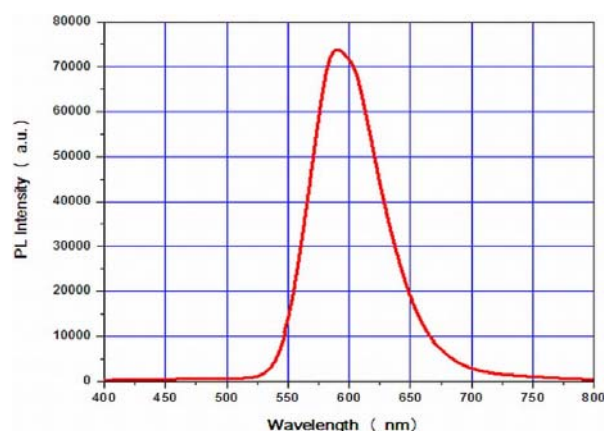


Fig. 5. Room-temperature photoluminescence spectrum of sonicated PbS nanoparticles.

### 5. Formation mechanism

In recent years ultrasonic irradiation has emerged as a novel energy source for the fabrication of nanoparticles. Its capability to drive various chemical reactions, such as reduction, oxidation, dissolution, decomposition [20] and polymerization [21] to proceed under ambient conditions, gives it a sovereign authority over traditional energy sources such as light, heat or ionizing radiation. It has been found that three different regions are formed during the sonochemical process [22] is as follows: (i) The inner environment (gas phase) of the collapsing bubble, where elevated temperature (several thousands of degrees) and pressure (hundreds of atmospheres) are produced; (ii) The interfacial region where the temperature is lower than that in the gas-phase region but still high enough to induce a sonochemical reaction and (iii) The bulk solution region, which is at ambient temperature (Fig. 6).

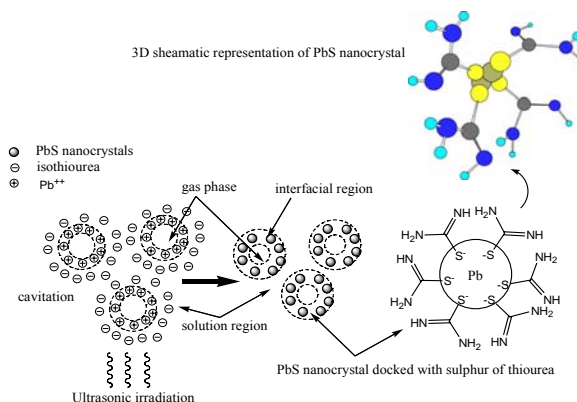
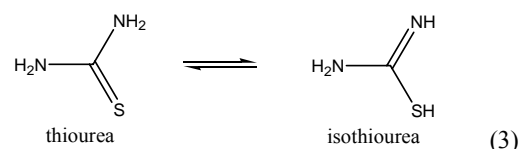
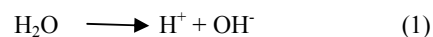


Fig. 6. Schematic presentation of the formation of PbS nanocrystals under ultrasonication irradiation.

Among the above-mentioned three regions, it seems that the current sonochemical reaction occurs within the interfacial region. If the reaction takes place inside the collapsing bubble, the product is amorphous as a result of the cooling rates ( $> 10^{10}$  K/s) [23], whereas if the reaction takes place at the interface, one expects to obtain crystalline product. The result can also be proved by the XRD pattern (Fig. 1) from which we can clearly see that the PbS nanoparticles synthesized by sonochemical method have high crystallinity.

The reaction steps and formation mechanism in the sonochemical process can be summarized as follows:



equations (1)–(3) represents the formation of primary ions by dissociation of water, lead acetate, and thiourea then PbS nanocrystals are formed according to reaction (4) –



This takes place under ultrasonic irradiation for 2 hour.

In order to clarify whether ultrasonic irradiation is an important step in PbS nanoparticle formation. We carried out a comparison experiment in the absence of ultrasonic irradiation under the same conditions. However, we could not obtain smaller nano-sized PbS nanoparticles and better crystallinity (Fig. 2).

## 6. Discussion

Up to now scientists have used different sulphur source as well as capping agents to synthesize and control the size of PbS nanoparticles. There has not been a consistent explanation on the mechanism of control of particle size using different capping agent. In our study we hypothesize the role of thiourea in controlling the size and its use as a sulphur source.

1. Thiourea isomerises in two tautomeric forms of thiourea and Isothiourea. C=S group in thiourea is difficult to perturb because the C=S bond distance is  $1.60 \pm 0.1 \text{ \AA}$ . Therefore, isothiourea form is probably the most suitable to provide sulphur source.

2. Thiourea molecules contain an active functional group which is similar to amide groups. This group can react easily with lead ions by chelation. Thiourea molecules themselves can bind each other through Van der Waals interaction and other weak bonds. Ultimately, the PbS nanoparticles come into being, which are made up of a PbS nanocrystal with sulphur docked in the crystal and the surrounding thiourea molecules (shown in Fig. 6).

3. This docking of thiourea sulphur inside the lead sulphide crystal not only provide sulfur for over all growth of crystal but also simultaneously control the particle size leading to quantum confinement of nanocrystal. Fig. 6 shows the probable process of growth of lead sulphide nanocrystals using thiourea under high energy ultrasonication irradiation.

## 7. Conclusion

In summary, a method to fabricate PbS nanocrystals have been developed. The PbS nanocrystals are synthesized from the reaction of Lead Acetate dihydrate and Thiourea. X-Ray diffraction pattern reveal cubic crystalline structure of synthesized PbS nanocrystals. The photoluminescence (PL) measurement show a sharp emission peak around 590 nm. Such a large blue shift from 0.41 eV (band gap of the bulk) to 2.11 eV (590 nm) indicates a significant amount of quantum confinement energy. This research could give rise to an alternative approach of producing PbS nanostructures and offer future studies for more information about PbS nanocrystals.

## Acknowledgement

This work was financially supported by Department of Science and technology (DST), Government of India.

## References

- [1] L. Bakueva, S. Musikhin, M. A. Hines, T.-W.F. Chang, M. Tzolov, G. D. Scholes, E. H. Sargent, *Appl. Phys. Lett.* **82**, 2895 (2003).

- [2] L. Bakueva, G. Konstantatos, L. Levina, S. Musikhin, E. H. Sargent: *Appl. Phys. Lett.* **84**, 3459 (2004).
- [3] V. L. Colvin, M. C. Schlamp, A. P. Alivisatos: *Nature*, **370**, 354 (1994).
- [4] D. L. Klein, R. Roth, A. K. L. Lim, A. P. Alivisatos, P. L. McEuen: *Nature*, **389**, 699 (1997).
- [5] P. B. Xie, W. P. Zhang, M. Yin, H. T. Chen, W. W. Zhang, L. R. Lou, S. D. Xia, *J. Colloid. Interface Sci.* **229**, 534 (2000).
- [6] A. P. Alivisatos: *Science* **271**, 933 (1996).
- [7] Y. Wang: *Acc. Chem. Res.* **24**, 133 (1991).
- [8] W. Chen, R. Sammynaiken, Y. Huang, J. O. Malm, R. Wallenberg, J. O. Bovin, V. Zwiller, N. A. Kotov, *J. Appl. Phys.* **89**, 1120 (2001).
- [9] A. A. R. Watt, D. Blake, J. H. Warner, E. A. Thomsen, E.L. Tavenner, R. Rubinsztein-Dunlop, P. Meredith: *Appl. Phys.* **38**, 2006 (2005).
- [10] R. K. Joshi, A. Kanjilal and H. K. Sehgal: *Appl. Surf. Sci.* **221**, 43 (2004).
- [11] R. Thielsch, T. B. Mohme, R. Reiche, D. SchlMafer, H. D. Bauer, H. B. Mottcher: *Nanostruct. Mater.* **10**, 131 (1998).
- [12] K. K. Nanda, F. E. Kruis, H. Fissan, M. Acet: *J. Appl. Phys.* **91**, 2315 (2002).
- [13] S. W. Lu, U. Sohling, M. Mennig and H. Schmidt: *Nanotechnology* **13**, 669 (2002).
- [14] C. Wang, W. X. Zhang, X. F. Qian, X. M. Zhang, Y. Xie, Y. T. Qian: *Mater. Lett.* **40**, 255 (1999).
- [15] Y. Wang, N. Herron: *J. Phys. Chem.* **95**, 525 (1991).
- [16] J. P. Yang, S. B. Qadri and B. R. Ratna: *J. Phys. Chem.* **100**, 17255 (1996).
- [17] S. W. Chen, A. Lindsay, J. Truax, M. Sommers: *Chem. Mater.* **12**, 3864 (2000).
- [18] A. A. Patel, F. X. Wu, Z. J. Zhang, L. Claudia, T. Martinez, R. K. Mehra, Y. Yang, S. H. Risbud: *J. Phys. Chem. B* **104**, 11598 (2000).
- [19] N. A. Dhas, Y. Kotypin, A. Gedanken: *Chem. Mater.* **9**, 3159 (1997).
- [20] K.S. Suslick: *Ultrasound: Its chemical, Physical and Biological Effects*, (VCH, Weinheim, 1988).
- [21] P. Kruus, M. O. Neil, D. Robertson: *Ultrasonics* **28**, 304 (1990).
- [22] K. S. Suslick, D. A. Hammerton, R. E. Cline: *J. Am. Chem. Soc.* **108**, 5641 (1986).
- [23] K. S. Suslick, S. B. Choe, A. A. Cichowlas, M. W. Grinstaff: *Nature* **353**, 414 (1991).

\*Corresponding author: vyomparashar@gmail.com